

# Preparation and Characterization of Silver, Magnesium & Bismuth Doped Titanium Dioxide Nanoparticles for Solar Cell Applications

K. M. Prabu<sup>1</sup>, P. M. Anbarasan<sup>1,2</sup>

<sup>1</sup>Department of Physics, Periyar University, Salem 636 011, Tamil Nadu, India

<sup>2</sup>Centre for Nanoscience and Nanotechnology, Periyar University, Salem - 636 011, Tamil Nadu, India

**Abstract:** Nanostructures Nobel methods have unusual physicochemical properties and biological activities compared to their bulk parent materials. Thus in recent years a number of physical, chemical and biological techniques were applied for the development of metal nanoparticles (NPs). This study aimed at developing superior quality TiO<sub>2</sub> based nanomaterials for photovoltaic applications, with the major contributions of this study being the following. Synthesis of Mg, Ag and Bi doped TiO<sub>2</sub> nanomaterials using an acid modified sol-gel technique. In this paper we investigate the optical absorption, functional group, surface morphology and elementary composition of pure TiO<sub>2</sub> and doped TiO<sub>2</sub> nanoparticles by using UV-Visible spectroscopy, FT-IR, Photoluminescence (PL) -Studies, FE-SEM and EDS analysis.

**Keywords:** Mg, Ag and Bi doped TiO<sub>2</sub> nanopowders and sol-gel method

## 1. Introduction

Nanoparticles have attracted great interest recently due to their unique physical and chemical properties, which are different from those of either the bulk materials or single atoms. Materials scientists are conducting research to develop novel materials with better properties, more functionality and lower cost than the existing one. Several physical, chemical methods have been developed to enhance the performance of nanomaterials displaying improved properties with the aim to have a better control over the particle size distribution [1-5]. Nanocrystalline TiO<sub>2</sub> has shown excellent performance by comparison to other semiconductors such as ZnO, SnO<sub>2</sub>, Ag, Mg, Mn, Bi and Nb<sub>2</sub>O<sub>5</sub>. Doping of TiO<sub>2</sub> nanomaterials has been investigated for more than 10 years [6-8]. Doping a metal or nonmetal into TiO<sub>2</sub> could change the band edge or surface states of TiO<sub>2</sub> [9]. Until now, most of the doping for TiO<sub>2</sub> nanomaterials has been explored for photo catalysis. The doping effects, however, do not seem so pronounced by comparison to the corresponding undoped TiO<sub>2</sub>. The energy conversion efficiency remained either unchanged or a little improvement. Over the past decade, nanomaterials have been the subject of enormous interest. Their defining characteristic is a very small size in the range of 1-100 nm. Due to their nanometer size, nanomaterials are known to have unique mechanical, thermal, biological, optical and chemical properties, together with the potential for wide-ranging industrial applications. Here, we synthesized nanocrystalline metal oxides through the sol-gel process [10-14]. The sol-gel process has become a widely used method during the last several decades. Basically the sol-gel process designates a type of solid materials synthesis procedure by chemical reactions in a liquid at low temperature. In a typical sol-gel process, independent solid colloidal particles ranging from 1 nm to 1 micrometer are formed from the hydrolysis and condensation of the precursors, which are usually inorganic metal salts or metal organic compounds such as metal alkoxides. It is usually easy to maintain such

particles in a dispersed state in the solvent, in which case a colloidal suspension also termed a sol is obtained. In the second step, these colloidal particles can be made to link with each other by further sol condensation, while they are still in the solvent, so as to build a three-dimensional open grid, termed gel. The transformation of a sol to a gel constitutes the gelation process compared with other methods, such as the solid-state method, Plasma Spraying, Solution Precipitation, Hydrothermal Method, solvothermal Synthesis etc. The advantage of using sol-gel process has a lot to offer in the area of applications. Since the sol-gel prepared catalytic materials always involve several components (active metal ions on the oxide support) or the introduction of dopants (metal or non-metal) into the oxide [15-18].

TiO<sub>2</sub> nanomaterials are one of the potential candidates for solar energy application due to TiO<sub>2</sub>'s unique optoelectronic and photochemical properties. Especially, as a photovoltaic performance to efficient energy conversion for solar irradiations, TiO<sub>2</sub> nanomaterials have been receiving a great deal of attention. TiO<sub>2</sub>, especially its anatase phase, has attracted much attention for its potential application in degradation of various environmental pollutants, both gaseous and liquid. However; its short comings include a large band gap (~3.2 eV) which causes most of the solar spectrum unutilized. To extend the optical absorption of TiO<sub>2</sub> to the visible region, various dopants have been added to the oxide to improve its solar efficiency [19-20].

## 2. Materials and Methods

### 2.1. Chemicals Used

Most of the Chemicals used in the research are standard chemicals that are normally available in the laboratory. The chemicals used in this study were titanium isopropoxide, silver nitrate, magnesium nitrate, bismuth oxide glacial

acetic acid, benzyl alcohol; absolute ethanol, acetyl acetone, and methanol were bought from Sigma-Aldrich. All the chemicals were used without further purification.

## 2.2. Sample preparation

Metal oxide nanoparticles attract great attention in recent years on account of their special electronic and chemical properties. In this paper, Ag, Mg and Bi-doped TiO<sub>2</sub> nanoparticles with high photo catalytic activity were synthesized by sol-gel method. The sol-gel method is a versatile process used for synthesizing various oxide materials because it allows very simple control of particle size and the experimental process.

### 2.2.1 Preparation of Modified TiO<sub>2</sub> Nanoparticle Nanocomposites

The Ag-doped TiO<sub>2</sub> NPs were prepared by an acid modified sol-gel method. In the first step, Silver nitrate 0.05 mol % were dissolved in 60 ml of deionized water at room temperature, followed by adding 5 ml of glacial acetic acid and in the second step 14 ml titanium isopropoxide was dissolved in 40 ml of anhydrous ethanol with constant stirring. Then, the two solutions were added drop-wise together within 2 hours under constant stirring. Subsequently, the obtained sol was stirred continuously for 3 hours and aged for 3 days at room temperature. As-prepared TiO<sub>2</sub> gels were dried for 12 hours at 80°C. The obtained solids were ground and finally calcined at 500°C for 2h (heating rate = 3°C/min). The undoped TiO<sub>2</sub> nanoparticle was prepared using the same method for comparative purposes. The undoped TiO<sub>2</sub>, Mg doped TiO<sub>2</sub> & Bi doped TiO<sub>2</sub> nanoparticle was prepared using the same method for comparative purposes.

## 3. Results and Discussion

### 3.1 UV-Visible Absorption spectroscopy

Absorption spectroscopies are powerful non-destructive techniques to explore the optical properties of semiconducting nanoparticles. The UV-visible spectrum of modified TiO<sub>2</sub> nanopowders was obtained to determine the relationship between the solar energy conversion efficiency and spectroscopic property. The UV-visible spectral studies of the pure TiO<sub>2</sub>, Ag-TiO<sub>2</sub>, Mg-TiO<sub>2</sub>, Bi-TiO<sub>2</sub> were carried out using Lambda 35 model UV-visible spectrometer in the range of 200 to 1100 nm. The photo absorption of modified TiO<sub>2</sub> in the visible-light region was stronger than that of pure TiO<sub>2</sub>. The modified TiO<sub>2</sub> nanopowders were calcined at 500°C the visible-light photo absorption is strongest and it produces high photocatalytic activity.

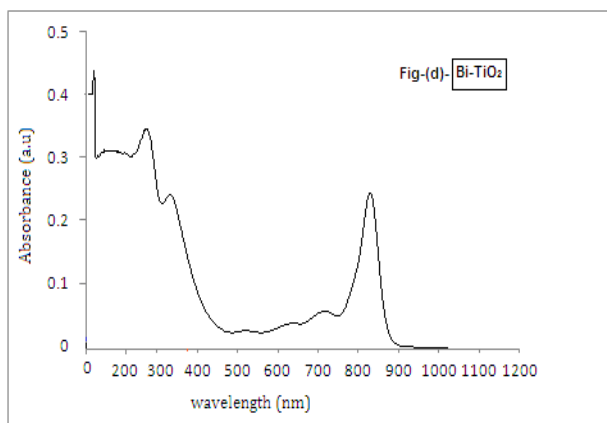
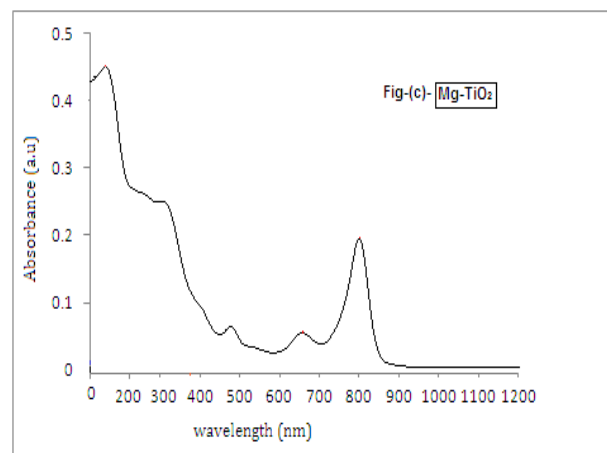
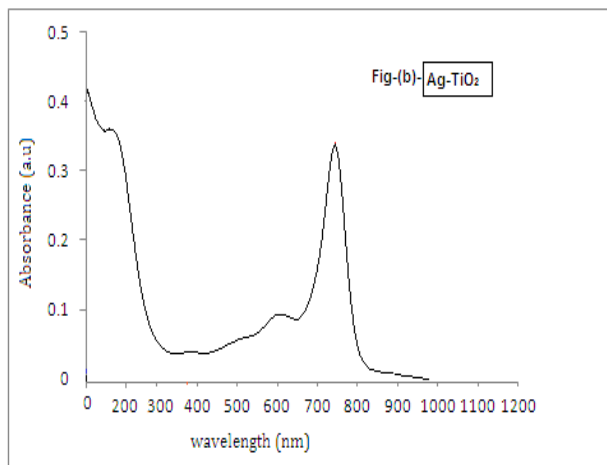
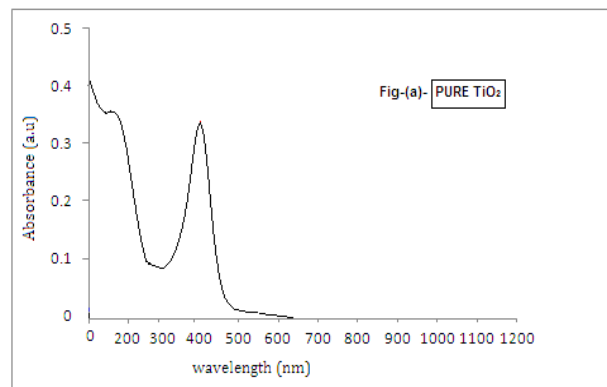


Figure 1: UV-visible spectra of (a) Pure TiO<sub>2</sub> (b) Ag-TiO<sub>2</sub> (c) Mg-TiO<sub>2</sub> (d) Bi-TiO<sub>2</sub>

**Table 1:** Measured Bandgap Energy of Synthesized TiO<sub>2</sub> Nanopowders (Bg-Bandgap value,  $\lambda_{\text{max}}$ -cutt-off wavelength)

Samples	$\lambda_{\text{max}}$ (nm)	Bg (eV)	$\lambda_{\text{max}}$ (nm)	Bg (eV)	$\lambda_{\text{max}}$ (nm)	Bg (eV)
Pure – TiO <sub>2</sub>	270	4.59	415	2.987	-	-
Ag-TiO <sub>2</sub>	340	3.646	600	2.066	731	1.696
Mg-TiO <sub>2</sub>	480	2.5829	640	1.937	806	1.538
Bi-TiO <sub>2</sub>	260	4.768	340	3.646	837	1.481

The energy gap ( $E_g$ ) is determined by the eq (1) [21],

$$E_g = 1239.8/\lambda \quad (1)$$

Where  $\lambda$  (nm) is the wavelength of the absorption edge in the spectrum. These results concluded that the Bi -TiO<sub>2</sub> nanopowders to the small band gap compare to other samples. The absorption spectrum of Bi doped TiO<sub>2</sub> shows that the small band gap in the entire visible region and it is a good candidate for solar cell applications. The energy gaps of modified TiO<sub>2</sub> shows mostly visible region and exhibits distinct synergistic effects as shown in the Table 1.

### 3.2 Fourier Transform Infrared Analysis (FT-IR)

The Fourier transform infrared (FTIR) Spectra of pure and various oxide doped TiO<sub>2</sub> nanopowders were recorded in the range of 4000 – 400 cm<sup>-1</sup> using KBr pellet technique Perkin Elmer spectrometer. The recorded FTIR spectrum of pure TiO<sub>2</sub>, Ag doped TiO<sub>2</sub>, Mg doped TiO<sub>2</sub> & Bi doped TiO<sub>2</sub> are shown in figure 2 (a), (b), (c), and (d) respectively. The different bonds and functional groups absorbed at different wavelengths, an infrared spectrum is used to determine the structure of organic molecules. Although this radiation is weak, it does supply sufficient energy for bonds in the molecule to vibrate by Stretching or Bending. The area from 3500 cm<sup>-1</sup> to 1300 cm<sup>-1</sup> is called the functional group region. The bands in this region are particularly useful in determining the type of functional groups present in the molecule. The area from 1300 cm<sup>-1</sup> to 667 cm<sup>-1</sup> is called the fingerprint region. A peak-by-peak match of an unknown spectrum with the spectrum of the suspected compound in this region can be used, much like a fingerprint, to conform its identity. The reaction between precursor materials of both pure and various oxide doped TiO<sub>2</sub> nanopowders are prepared by sol-gel method. The absorption band was observed in the range 3450.23-3388.62 cm<sup>-1</sup> for bare and various oxide doped TiO<sub>2</sub> nanoparticles, which was described to the both symmetric and asymmetric stretching vibrations of the hydroxyl group. Whereas, the characteristic peaks between 1650-1700 cm<sup>-1</sup> is associated with the O-H banding vibration of the absorbed water molecules. The C-H bending is observed at 1370-1420 cm<sup>-1</sup> in the compound type of alcohols present in both samples. In the spectrum of pure TiO<sub>2</sub>, the peak at 480.55 cm<sup>-1</sup> should be attributed to Ti-O bond in the TiO<sub>2</sub> lattice (anatase titanium). For various oxide doped TiO<sub>2</sub> nanoparticles such as Mg, Ag, Bi & pure TiO<sub>2</sub> nanoparticles, the peaks locked in the region 580.24-620.18 cm<sup>-1</sup> indicating the Ti-O-O band. The bands between 728.77-657.25 cm<sup>-1</sup> illustrate the Ti-O-Ti stretching vibration. The weak bands between 2927.51-2920.55 cm<sup>-1</sup> and 2849.32-2835.60 cm<sup>-1</sup> could be described to the

characteristic frequencies of residual organic species assigned to C-H stretching vibrations of alkane groups.

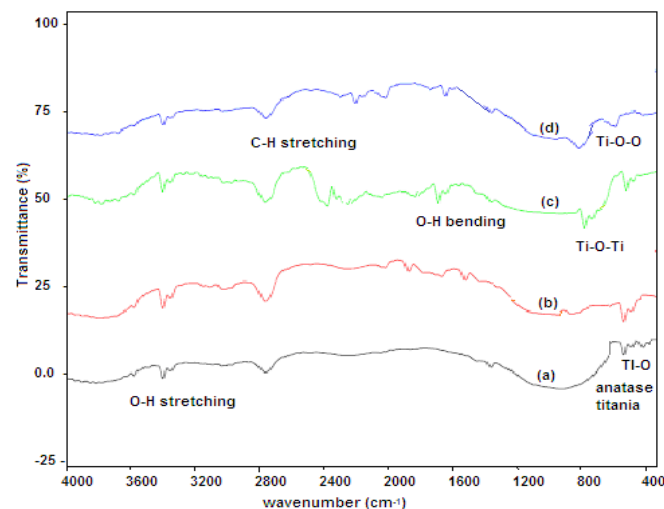


**Figure 2:** FT-IR spectra of (a) Pure TiO<sub>2</sub> (b) Ag-TiO<sub>2</sub> (c) Mg-TiO<sub>2</sub> (d) Bi-TiO<sub>2</sub>

### 3.3 Photo Luminescent (PL) studies

Photoluminescence emission spectra of Pure TiO<sub>2</sub>, Ag doped TiO<sub>2</sub>; Mg doped TiO<sub>2</sub> & Bi doped TiO<sub>2</sub> are shown in Fig 3 (a), (b), (c) & (d) respectively. The PL emission spectra exhibits emission peaks range of 200 nm -600 nm. In the PL characteristics of pure TiO<sub>2</sub> nanoparticles to display a blue photoluminescence band width strong intensity and sharp features centered at approximately 390 nm. The PL characteristics of Ag, Mg & Bi doped TiO<sub>2</sub> nanoparticles to display a strong intensity band width and broad features centered at approximately 420 nm, 450nm & 480 nm respectively. It exhibits a green luminescence and it is frequently attributed to bulk defects, such as dislocations and stacking faults, and deep-level traps. The bulk defects were not found in modified TiO<sub>2</sub> nanoparticles. The green-shifted emission was then ascribed to the bandgap reduction of TiO<sub>2</sub> due to its high density of states close to the conduction band minimum and the subsequent filling of conduction band edge by additional depended material induced carriers. The emission band present at 480 nm is known as green emission of Bi doped TiO<sub>2</sub> nanopowder. There are several explanations about the origin of green emission band. They may be due to i) recombination of free electrons from conduction band with holes captured on an acceptor level, ii) recombination of trapped electrons from a donor level with free holes and iii) recombination of electrons from a donor level with holes trapped on an acceptor level. The green band emission in the present study may be due to the acceptor levels related to interstitial bismuth oxide and donor levels due to native defects mostly occur in Bi doped TiO<sub>2</sub> powder.

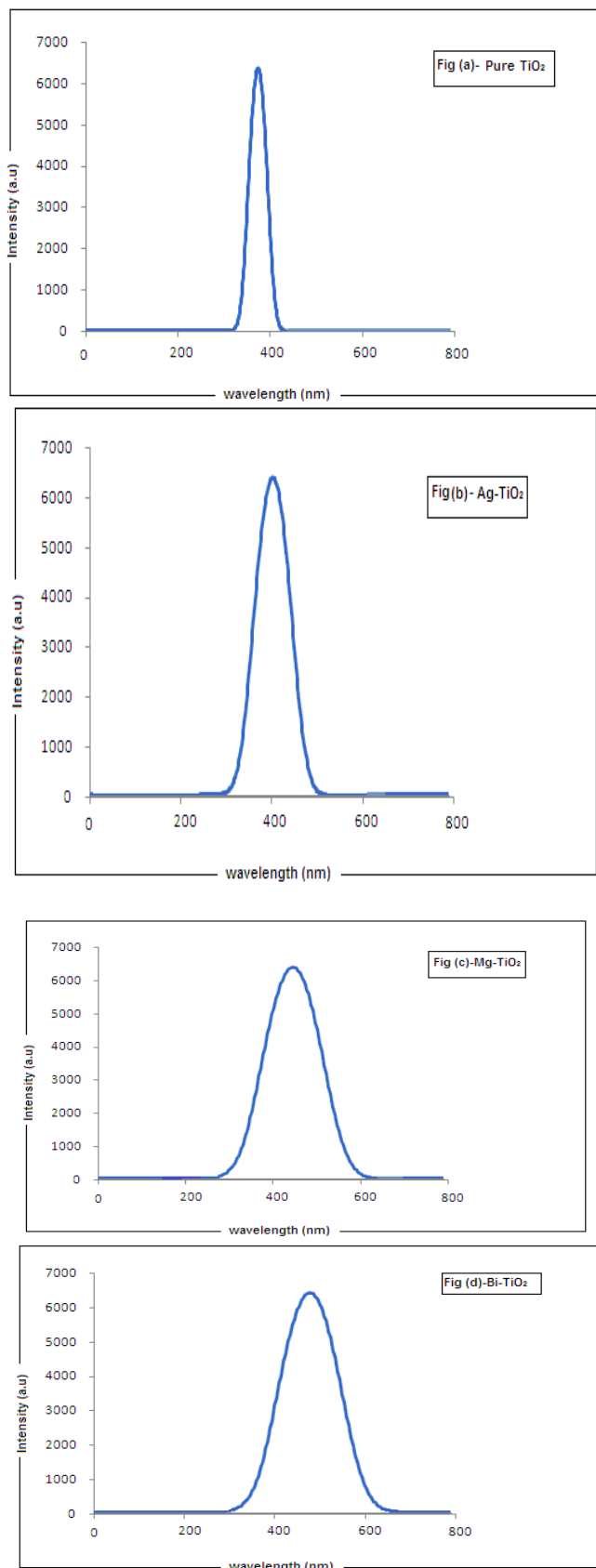


**Figure 3:** PL-studies of (a) Pure TiO<sub>2</sub> (b) Ag-TiO<sub>2</sub> (c) Mg-TiO<sub>2</sub> (d) Bi-TiO<sub>2</sub>

### 3.4 Field Emission Scanning Electron Microscopy (FE-SEM) Analysis

Figure 4 shows the FESEM micrographs of the pure and doped TiO<sub>2</sub> nanoparticles prepared by acid modified sol-gel

method. It has been observed that the TiO<sub>2</sub> nanoparticles annealed at 500°C were almost reveals that the primary particles are quite uniform in size, quite clean and roughly spherical in shape, and that the agglomerates are fused together to form comparatively smaller irregular grains giving rise to highly porous materials which enhancing the photovoltaic performance. The FE-SEM micrographs of the pure TiO<sub>2</sub> nanoparticles depicted in figure (a) has non-uniform distribution of spherical particles.

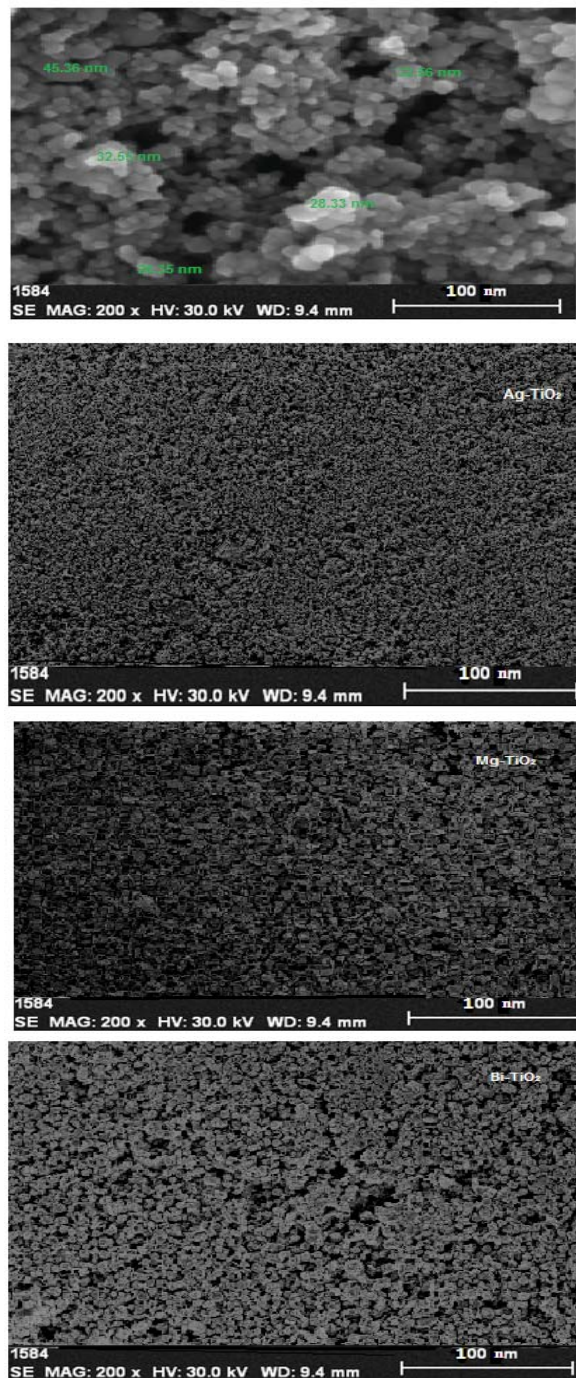


**Figure 4:** FESEM Micrographs (a) Pure TiO<sub>2</sub> (b) Ag-TiO<sub>2</sub> (c) Mg-TiO<sub>2</sub> (d) Bi-TiO<sub>2</sub>

### 3.5 EDS Analysis

The semi quantification of elemental analyses to identify the weight percentage of major and minor elements present in the samples were done using Energy Dispersive X-ray Spectrometer (EDS), JEOL model, JSD-5610 LV with an

accelerating voltage of 20KV. The result of energy dispersive X-ray spectroscopic (EDS) analysis of pure TiO<sub>2</sub> and doped TiO<sub>2</sub> nanopowders are shown in fig 5(a) & 5 (b, c & d). Trace elements are estimated by determining the percentage abundance of elements such as Ti, O & Zn present in the sample. In pure TiO<sub>2</sub> the concentration of titanium is 89.20% and the concentration of oxygen is 10.80% this result gives to the titanium and oxygen presents in sample.

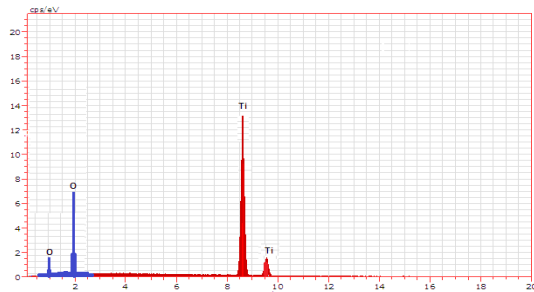


Figure 5 (a)

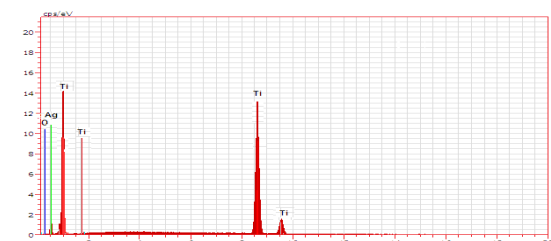


Figure 5 (a)

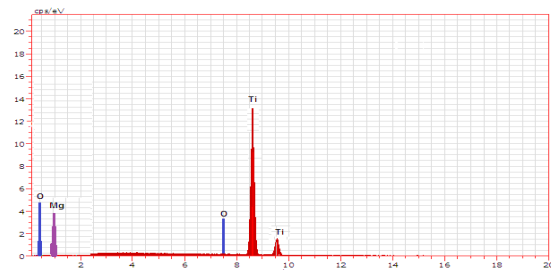


Figure 5 (c)

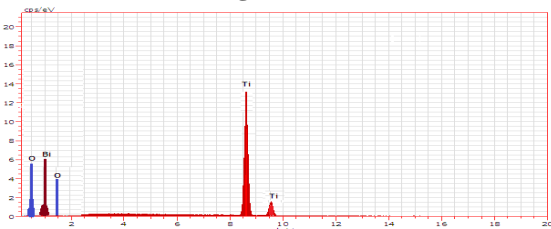


Figure 5 (d)

Figure 5: EDS Analysis (a) Pure TiO<sub>2</sub> (b) Ag-TiO<sub>2</sub> (c) Mg-TiO<sub>2</sub> (d) Bi-TiO<sub>2</sub>

Table 2 (a)

Sample	Element	Weight (%)	Atomic (%)
Pure TiO <sub>2</sub>	O K	32.16	61.40
	Ti K	67.84	38.60
	Total	100.00	100.00

Table -2 (b)

Sample	Element	Weight (%)	Atomic (%)
Ag- TiO <sub>2</sub>	O K	35.25	63.60
	Ti K	61.45	34.25
	Ag K	3.30	2.15
	Total	100.00	100.00

Table -2 (c)

Sample	Element	Weight (%)	Atomic (%)
Mg- TiO <sub>2</sub>	O K	36.34	65.55
	Ti K	59.40	31.30
	Mg K	4.26	3.15
	Total	100.00	100.00

Table 2 (d)

Sample	Element	Weight (%)	Atomic (%)
Bi- TiO <sub>2</sub>	O K	33.55	62.33
	Ti K	60.23	33.42
	Bi K	6.22	4.25
	Total	100.00	100.00

Table 2: EDS Analysis (a) Pure TiO<sub>2</sub> (b) Ag-TiO<sub>2</sub> (c) Mg-TiO<sub>2</sub> (d) Bi-TiO<sub>2</sub>

#### 4. Conclusions

The pure and doped TiO<sub>2</sub> nanoparticles were successfully prepared by sol-gel method. The UV-Visible and PL result shows doped titanium nanoparticles extend the absorption edge to the visible light range and make the red shift more distinct and also analyses the band gap value. The Ti-O bond of anatase phase in all the synthesized samples was identified by FT-IR measurements. The FE-SEM analysis reveals that the morphology of doped TiO<sub>2</sub> was smooth and well defined spherical shape with grain size 25-50 nm with minimal agglomeration compare to pure TiO<sub>2</sub>. Also analyses the morphology of doped TiO<sub>2</sub> was regular arrangement, spherical shape, uniform size, and good packing density. The doped and pure elements are identified from EDX spectrum, in which the spectrum confirms the elemental compositions of presented samples.

#### References

- [1] S. Shibata, K. Aoki, T. Yano and M. Yamane, Journal of sol-gel science and Technology, 11, 279, (1998).
- [2] H. Hahn, Nanostructured Materials, 9, 3, (1997).
- [3] H. Cheng, J. Ma, Z. Zhao, L. Qi, Chem. Mater., 7, (1995).
- [4] A. C. Jones, P. R. Chalker, J. Phys. D: Appl. Phys., 36, 80, (2003).
- [5] W.N. Wang, I. W. Lenggono, Y. Terashi, T. O. Kim, K. Okuyama, Mat. Sci.Eng. B, 123, (2005).
- [6] J. Yang, S. Mei, J. M. F. Ferreira, Mater. Sci. Eng. B, C15, (2001).
- [7] O. Carp, C. L. Huisman, A. Reller, Progress in Solid State Chem., 32, 33, (2004)
- [8] C. S. Kim, K. Okuyama, K. Nakaso, M. Shimada, Direct measurement of nucleation and growth modes in titania nanoparticles generation by a CVD method, J Chem Eng Jpn, 37(11), 1379, (2004).
- [9] Y. Cao, W. Yang, W. Zhang, G. Liub, P. Yue, Improved photocatalytic activity of Sn<sup>4+</sup> doped TiO<sub>2</sub> nanoparticulate films prepared by plasma-enhanced

- chemical vapor deposition. *New. J. Chem*, 2 (8), 218 – 222, (2004).
- [10] F. Gracia, J. P. Holgado, A. Caballero, A. R. Gonzalez-Elipe, Structural, Optical, and Photoelectrochemical Properties of Mn<sup>+</sup>-TiO<sub>2</sub> Model Thin Film Photocatalysts, *J. Phys. Chem. B*, 108 (45), 17466-17476, (2004).
- [11] T. S. Sudarshan, In Coated powders - new horizons and applications, *Advances in Surface Treatment: Research & Applications (ASTRA), Proceedings of the International Conference, Hyderabad, India*, 412-422, (2003).
- [12] C. Kim, K. Nakaso, B. Xia, K. Okuyama, M. Shimada, A New Observation on the Phase Transformation of TiO<sub>2</sub> Nanoparticles Produced by a CVD Method, *Aerosol Science & Technology*, 39 (2), 104-112, (2005).
- [13] C. Liang, Y. Shimizu, T. Sasaki, N. Koshizaki, Synthesis, characterization, and phase stability of ultrafine TiO<sub>2</sub> nanoparticles by pulsed laser ablation in liquid media, *J Mater Res*, 19 (5), 1551-1557, (2004).
- [14] K. Nagaveni, M. S. Hegde, G. Madras, Structure and Photocatalytic Activity of Ti<sub>1-x</sub> MxO<sub>2</sub>; (M = W, V, Ce, Zr, Fe, and Cu) Synthesized by Solution Combustion Method. *J. Phys. Chem. B*, 108 (52), 20204-20212, (2004).
- [15] K. Jinsoo, L. Jae Won, L. Tai Gyu, N. Suk Woo, H. Jonghee, Nanostructured titania membranes with improved thermal stability, *Journal of Materials Science*, 40 (7), 1797-1799, (2005).
- [16] M. Iwasaki, S. A. Davis, S. Mann, Spongelike Macroporous TiO<sub>2</sub> Monoliths Prepared from Starch Gel Template, *J Sol-Gel Sci Techn*, 32, 99-105, (2004).
- [17] D. V. Bavykin, J. M. Friedrich, F. C. Walsh, Protonated Titanates and TiO<sub>2</sub> Nanostructured Materials: Synthesis, Properties, and Applications, *Advanced Materials*, 18 (21), 2807-2824, (2006).
- [18] A. C. Jones, P. R. Chalker, *J. Phys. D: Appl. Phys.*, 36, 80, (2003).
- [19] K. L. Choy, *Prog. Mater. Sci.*, 48, 164, (2003).
- [20] R. Van de Krol, A. Goossens, J. Schoonman, *J. Electrochem. Soc.*, 144, (1997).
- [21] M. Fernandez-Garcia, A. Martinez-Arias, J. C. Hanson, J. A. Rodriguez, *Nanostructured Oxides in Chemistry: Characterization and Properties. Chem. Rev.*, 104, (9), 4063-4104, (2004).